International Journal of Applied Mechanics

Uni-axial non-linear stress-strain modelling of multi-layer elastomer silicone composites

Annemie Van Hirtum
Univ. Grenoble Alpes, CNRS, Grenoble INP, LEGI, France

Anna Ines Fernández
Dept. of Materials Science and Physical Chemistry, Univ. of Barcelona, Spain

Xavier Pelorson
Univ. Grenoble Alpes, CNRS, Grenoble INP, LEGI, France

Received date
Accepted date

The recently proposed one-parameter ExpCub procedure (Ahmad *et al.* [2023]) allows to predict stress-strain curves covering the linear (up to 0.3) and non-linear (up to 1.5) strain region of multi-layer elastomer silicone composites as a function of their effective low-strain Young's modulus (up to 65 kPa). Therefore, the procedure is of potential interest for multi-layer silicone composite design as it limits the need for experimental data. In this work, performance statistics of the ExpCub procedure are compared to those obtained for best fit reference models depending on one (neo-Hookean), two (Yeoh, Gent, Odgen, Mooney-Rivlin, exponential and cubic relationships) or more (Pucci-Saccomandi, Yeoh, Odgen, Criscone, generalized Mooney-Rivlin) model parameters. It is found that the predictive one-parameter ExpCub procedure and the best fit one-parameter neo-Hookean model result in a similar accuracy considering the coefficient of determination, e.g. median value 95% or more. It is further observed that the accuracy (coefficient of determination 99.9%) of best fit curves obtained for two-parameter exponential and cubic relationships, underlying the ExpCub procedure, competes with the overall best accuracy observed for multi-parameter models such as the Yeoh model with two or three parameters. These findings are confirmed considering the Akaike or Bayesian information criterion for model selection. Therefore, it is concluded that the ExpCub procedure is efficient as well as accurate, which confirms its interest as a predictive model for the non-linear stress-strain behaviour of elastomer silicone composites.

Keywords: Elastomer silicone composites; Non-linear stress–strain modelling; Model performance statistics; Vocal fold biomaterial

1. Introduction

Molded multi-layer elastomer silicone composites (SCs) are of interest for a wide range of applications. For example, in the context of soft tissue engineering for biomaterials, they allow to mimic the multi-layer anatomical vocal fold structure in physical studies of the fluid-structure interaction that drives vocal fold auto-oscillation during voice production [Murray and Thomson, 2012; Tokuda and Shi-

mamura, 2017; Bouvet *et al.*, 2020]. Nevertheless, their *a-priori* non-linear stress-strain behaviour, and thus certainly their optimal stress-strain design, may be hampered by the lack of a predictive model. It follows that currently the stress-strain behaviour of SCs needs to be determined from mechanical tension testing. This often requires a laborious process involving trial-and-error molding and subsequent testing, which limits the usefulness of SCs in systematic parametric studies of the influence of stress-strain behaviour on physical phenomena *e.g.*, driven by fluid-structure-interaction.

To help solve this problem, recently Ahmad *et al.* [2023] proposed an analytical one-parameter non-linear stress-strain model approach for molded elastomer-based SCs under uni-axial tension load for strains up to 1.5, corresponding to elongations up to 350%. This approach, for convenience labelled the ExpCub procedure and detailed in Section 3, depends only on the effective low-strain Young's modulus ($\mathcal{E}_{eff}$) characterising the elastic low-strain region, which for assessed elastomer-based SCs coincides with strains up to 0.3 [Ahmad *et al.*, 2023; Van Hirtum *et al.*, 2023]. For these SCs, $\mathcal{E}_{eff}$ (up to 65 kPa) is either obtained from experimental characterisation under low-strain tension load or estimated analytically considering homogenised SCs in the case that multi-layer stacking characteristics (geometry, positioning and Young's modulus of each layer in the stack) are known [Ahmad *et al.*, 2021, 2022]. As a result, the ExpCub procedure is efficient in reducing or eliminating the need for experimental characterisation and thus in accounting for the non-linear stress-strain behaviour from the SCs design stage onward. To explore the potential of the ExpCub procedure beyond its efficiency for SC's design and selection, in this work, its accuracy is compared with best fits obtained from reference hyperelastic constitutive models for isotropic, homogeneous and incompressible elastic materials under uni-axial tension. Reference models with one, two or more parameters are considered as outlined in Section 2 since models with three or more parameters are known to improve the accuracy [Destrade *et al.*, 2017]. Assessed stress-strain datasets on 22 SCs are summarised in Appendix A. Quantified model accuracy measures (coefficient of determination R^2 or adjusted coefficient of determination R_a^2) and information criteria for model selection (Akaike AICc or Bayesian BIC) are outlined in Appendix B. Statistics of these model performance measures on assessed datasets are compared and discussed in Section 4. A conclusion is formulated in Section 5.

2. Hyperelastic reference models for uni-axial tension

2.1. *Basic equations for uni-axial stress-strain behaviour*

For an incompressible material with initial length l_0 and initial cross-sectional area $\mathcal{A}_0$ subjected to an uni-axial force $\mathcal{F}$ resulting in elongation Δl along the force

direction, true stress σ_t and true strain ε_t are given as

$$\sigma_t = \frac{\mathcal{F}}{\mathcal{A}} \qquad \text{and} \qquad \varepsilon_t = \ln\left(\frac{l}{l_0}\right), \tag{1}$$

with $l = l_0 + \Delta l$ and $\mathcal{A}$ indicating respectively the length and the area of the material after deformation, the latter quantity being obtained as $\mathcal{A} = \mathcal{A}_0\, l_0/l$ according to volume conservation [Ahmad *et al.*, 2021]. For strains $\varepsilon_t \leq \varepsilon_l$, SCs exhibit low-strain linear elastic stress-strain behaviour characterised by an effective Young's modulus $\mathcal{E}_{eff}$ corresponding to the linear slope of the stress-strain curve so that

$$\mathcal{E}_{eff} = \frac{\sigma_t}{\varepsilon_t}. \tag{2}$$

For strains $\varepsilon_t > \varepsilon_l$, the stress-strain relationship becomes non-linear until potentially a high-strain linear region is reached [Ahmad *et al.*, 2023; Van Hirtum *et al.*, 2023].

Continuous non-linear hyperelastic constitutive stress-strain models account for the linear low-strain onset characterised by $\mathcal{E}_{eff}$, the subsequent non-linear region and a potential linear region of high strain. When considering homogeneous deformations and homogeneous strain, deformations are of the form

$$x_1 = \lambda_1 X_1, \;\; x_2 = \lambda_2 X_2, \;\; x_3 = \lambda_3 X_3, \tag{3}$$

with Cartesian material coordinates (X_1, X_2, X_3), spatial deformation coordinates (x_1, x_2, x_3) along the same axes and principal deformation stretches λ_1, λ_2 and λ_3. Setting $\lambda_1 = \lambda$, the incompressibility constraint $\lambda_1\,\lambda_2\,\lambda_3 = 1$ gives $\lambda_2 = \lambda_3 = \lambda^{-\nu}$ with generalised Poisson ratio $\nu = 0.5$. Further applying the assumption of isotropy, shear modulus μ relates to $\mathcal{E}_{eff}$ as

$$\mu = \frac{\mathcal{E}_{eff}}{2(1+\nu)}, \tag{4}$$

so that for $\nu = 0.5$

$$\mu = \mathcal{E}_{eff}/3. \tag{5}$$

Under these conditions, the strain invariants become either function of λ or take on a constant value as

$$I_1 = \lambda^2 + \frac{2}{\lambda}, \;\; I_2 = \frac{1}{\lambda^2} + 2\lambda, \;\; I_3 = 1. \tag{6}$$

Strain energy density function W is defined as the materials strain energy per unit volume expressing the work done by the load or

$$W(\lambda) = \int_1^{\lambda} \frac{\sigma_t(\lambda)}{\lambda} d\lambda, \tag{7}$$

with elongation $\lambda \geq 1$ and $\lambda = e^{\varepsilon_t}$. Consequently, for an incompressible material and considering Eq. (6), the stress-strain relationship for uni-axial tension is derived from $W(\lambda)$ or $W(I_1, I_2)$ when expressed as a function of the strain invariants following

$$\sigma_t = 2\big(\lambda^2 - \lambda^{-1}\big)\left(\frac{\partial W}{\partial I_1} + \lambda^{-1}\frac{\partial W}{\partial I_2}\right). \tag{8}$$

In the next Section 2.2, the strain energy density function W for reference constitutive hyperelastic stress-strain models is given. The number of model parameters M is indicated.

2.2. *Reference hyperelastic stress-strain models for uni-axial tension*

In this section, hyperelastic stress-strain reference models with a different number of parameters $M \geq 1$, and thus a different model complexity, are presented [Ogden, 1997; Fu and Ogden, 2001; Lemaitre, 2001; Taber, 2004; Odgen *et al.*, 2004; Drozdov and Gottlieb, 2006; Fung, 2010; Marckmann and Verron, 2006]. As the ExpCub procedure relies on one parameter, comparison with the reference one-parameter ($M = 1$) model described in Section 2.2.1 is essential. Comparison with two-parameter models is pertinent since the ExpCub procedure is derived from mathematical two-parameter ($M = 2$) relationships, *i.e.*, two-parameter exponential and cubic relationships detailed in Section 4.3. For completeness, also more complex multi-parameter ($M \geq 3$) models are assessed.

2.2.1. *The one-parameter neo-Hookean model, $M = 1$*

The neo-Hookean (nH) hyperelastic model is a one-parameter model ($M = 1$) obtained as a limit case of the thermodynamically based Arruda-Boyce model [Arruda and Boyce, 1993; Ogden, 1997; Gent, 2012]. It has thus the advantage of following from a physics-based mechanistic model. For an incompressible material, the strain energy density function depends on the first strain invariant I_1 only as

$$W(I_1) = \frac{\mu}{2}\big(I_1 - 3\big). \tag{9}$$

Shear modulus μ in the natural or undeformed stress-free configuration can thus be estimated by fitting Eq. (9) to measured stress-strain data.

2.2.2. *The multi-parameter Yeoh model, $M \geq 1$*

The truncated strain energy density function of the Yeoh (Y) polynomial model [Yeoh, 1993] depends on the first strain invariant I_1 as

$$W(I_1) = \sum_{i=1}^{M} C_i (I_1 - 3)^i \tag{10}$$

with $M \geq 1$ unknown parameters and (C_i) material constants. The initial shear modulus is obtained as $\mu = 2C_1$. For $M = 1$, Eq. (10) reduces to Eq. (9) associated with the one-parameter neo-Hookean model.

2.2.3. *The two-parameter Gent model, $M = 2$*

The Gent (G) model is a two-parameter model ($M = 2$) [Gent, 1996], reflecting the behaviour of molecular models based on Langevin statistics, for which the strain energy density function is given as

$$W(I_1) = \frac{\mu}{2} J_m \log\left(1 - \frac{I_1 - 3}{J_m}\right) \tag{11}$$

with the two-parameter set (μ, J_m) indicating shear modulus μ and stiffening parameter $J_m > 0$. It is generally assumed that $J_m \gg 1$ as it indicates the upper limit of strain invariant I_1 and $I_1 < 3 + J_m$ indicating limiting chain extensibility in molecular-based models. For $J_m \to \infty$, Eq. (11) reduces to the neo-Hookean model of Eq. (9). The model is often used to describe rubber elasticity as it represents well material stiffening at large strains.

2.2.4. *The three-parameter Pucci-Saccomandi model, $M = 3$*

A three-parameter (μ, J_m, C_2) extension of the Gent model is the Pucci-Saccomandi (PS) model [Pucci and Saccomandi, 2002], and thus also a limiting chain extensibility model, characterised by

$$W(I_1, I_2) = \frac{\mu}{2} J_m \log\left(1 - \frac{I_1 - 3}{J_m}\right) + C_2 \log\left(\frac{I_2}{3}\right) \tag{12}$$

where the additional parameter in the second term indicates the contribution of I_2. For $C_2 = 0$, Eq. (12) reduces to Eq. (11) of the Gent model.

2.2.5. *The multi-parameter Odgen model, $M \geq 2$*

The series expansion characterising the strain energy density function of the phenomenological multi-parameter Odgen (O) model [Ogden, 1997; Odgen *et al.*, 2004]

restricted to a finite number of terms $L \geq 1$ is given as

$$W(\lambda) = \sum_{i=1}^{L} \frac{\mu_i}{\alpha_i} \left(\lambda^{\alpha_i} + 2\lambda^{-\alpha_i/2} - 3 \right) \tag{13}$$

with $M = 2L \geq 2$ unknowns from L two-parameter sets (μ_i, α_i), which are material constants satisfying the requirements

$$\sum_{i=1}^{L} \mu_i \alpha_i = 2\mu \qquad \text{and} \qquad \mu_i \alpha_i > 0. \tag{14}$$

2.2.6. *The multi-parameter Criscone model, $M \geq 3$*

The Criscone (C) model [Criscione *et al.*, 2000] relies on invariants K_1, K_2 and K_3 of the natural or Hencky strain with principal values $(\ln \lambda_1, \ln \lambda_2, \ln \lambda_3)$. For an incompressible and isotropic material under uni-axial tension, the truncated series expansion of the strain energy function with $L \geq 3$ reads

$$W(K_2, K_3) = \sum_{i=2}^{L} \frac{1}{i} \gamma_{i-1} K_2^i + K_3 \sum_{j=3}^{L} \xi_j K_2^j \tag{15}$$

as a function of the stretches

$$K_2 = \frac{\sqrt{6}}{2} \ln \lambda \quad \text{and} \quad K_3 = 1 \tag{16}$$

for $M = 2L - 3$ terms and unknown parameters $(\gamma_1, \ldots, \gamma_{L-1}, \xi_3, \ldots, \xi_L)$.

2.2.7. *The two-parameter Mooney-Rivlin model, $M = 2$*

The strain energy density function for the two-parameter Mooney-Rivlin (MR) model [Mooney, 1940; Rivlin, 1948; Boulanger and Hayes, 2001] is given as

$$W(I_1, I_2) = C_1(I_1 - 3) + C_2(I_2 - 3) \tag{17}$$

with two unknown ($M = 2$) material constants C_1 and C_2. The initial shear modulus is given as $\mu = 2(C_1 + C_2)$. For $C_2 = 0$, Eq. 17 reduces to the one-parameter neo-Hookean model as $\mu = 2C_1$.

2.2.8. *The multi-parameter generalized Mooney-Rivlin model, $M \geq 3$*

Several models are based on a series expansion so that in general a polynomial generalized Mooney-Rivlin (gMR) model (or polynomial hyperelastic model) is of

interest [Bower, 2009]. In this case the strain energy density function is given by a truncated series expansion with $L \geq 1$ as

$$W(I_1, I_2) = \sum_{i,j=0}^{L} C_{ij}(I_1 - 3)^i (I_2 - 3)^j \tag{18}$$

with $C_{00} = 0$ and thus $M = (L+1)^2 - 1$ unknown parameters C_{ij} denoting material constants. The initial shear modulus is obtained as $\mu = 2(C_{01} + C_{10})$. For $L = 1$ and imposing $C_{00} = 0$ and $C_{11} = 0$, Eq. 18 reduces to the two-parameter Mooney-Rivlin model with $C_1 = C_{10}$ and $C_2 = C_{01}$. Consequently, when in addition $C_{01} = C_2 = 0$ holds, Eq. (18) coincides with the one-parameter neo-Hookean model.

3. One-parameter ExpCub procedure for SCs, $M = 1$

The rapid non-linear increase of stress-strain curves measured on elastomer SC specimens [Ahmad *et al.*, 2023; Van Hirtum *et al.*, 2023] (seeA) is also observed for soft biological tissues [Alipour and Titze, 1991; Odgen *et al.*, 2004; Gou, 1970; Fung, 1967, 2010; Demiray, 1972; Zhang *et al.*, 2006; Tanaka *et al.*, 2011; Burks *et al.*, 2020]. In line with the qualitative description of this behaviour, *'an exponential toe followed by a linear elastic region'* [Fung, 1967; Alipour and Titze, 1991; Tanaka *et al.*, 2011], a two-parameter (A, B) non-linear exponential stress-strain relationship,

$$\text{exponential: } \sigma_t(\varepsilon_t; A, B) = A\,(e^{B\,\varepsilon_t} - 1), \tag{19}$$

is used since the pioneering work of Fung [Fung, 1967]. Additionally, and following the use of a third order or cubic polynomial stress-stain relationship in previous works [Alipour and Titze, 1991; Saccomandi *et al.*, 2022], it was shown for the SCs of interest [Ahmad *et al.*, 2023] that a two-parameter (a, b) cubic relationship,

$$\text{cubic: } \sigma_t(\varepsilon_t; a, b) = a\,\varepsilon_t^3 + b\,\varepsilon_t, \tag{20}$$

provides a near match to the exponential relationship in Eq. (19) for strains up to 1.5 ($\varepsilon_t \leq 1.5$) corresponding to specimen elongations up to 350%. Consequently, both the exponential and cubic two-parameter relationship provide accurate estimations of measured SCs stress-strain curves as coefficients of determination (Eq. (B.1)) associated with the best fit accuracies yield $R^2 > 99\%$ for both relationships [Ahmad *et al.*, 2023; Van Hirtum *et al.*, 2023]. Estimated best fit two-parameter sets are denoted $(\hat{A}, \hat{B})$ for the exponential and $(\hat{a}, \hat{b})$ for the cubic stress-strain relationship.

The near match of both Eq. (19) and Eq. (20) in this strain range ($\varepsilon_t \leq 1.5$) is exploited in [Ahmad *et al.*, 2023] to analytically model expressions (Modelled

parameter sets, suffix -M) for the exponential (Eq. (19)) and cubic (Eq. (20)) two-parameter sets. The modelled two-parameter sets are given as:

$$\text{exponential (E-M): } (\tilde{A}, \tilde{B}) \approx (\mathcal{E}_{eff} \,/\, 2.15,\, 2.15), \tag{21a}$$

$$\text{cubic (C-M): } (\tilde{a}, \tilde{b}) \approx (2.53\,\mathcal{E}_{eff},\, \mathcal{E}_{eff}). \tag{21b}$$

The linear low-strain stress-strain behaviour in terms of these modelled parameters is then expressed as $\tilde{A}\,\tilde{B} \approx \mathcal{E}_{eff}$ and $\tilde{b} \approx \mathcal{E}_{eff}$ for the exponential and cubic relationship respectively. These modelled parameter expressions (Eq. (21)) are either constant (*i.e.*, for $\tilde{B}$) or proportional to $\mathcal{E}_{eff}$ (*i.e.*, for $\tilde{A}$, $\tilde{a}$ and $\tilde{b}$). Fitting these functions to a subset of overall best fit parameters estimated on measured SCs stress-strain datasets leads to the following data-based approximations for the exponential (Eq. (19)) and cubic (Eq. (20)) two-parameter set approximations (Data-Based parameter sets, suffix -DB) [Ahmad *et al.*, 2023]:

$$\text{exponential (E-DB): } (\hat{\tilde{A}}, \hat{\tilde{B}}) \approx (\mathcal{E}_{eff} \,/\, 3.03,\, 2.21), \tag{22a}$$

$$\text{cubic (C-DB): } (\hat{\tilde{a}}, \hat{\tilde{b}}) \approx (1.78\,\mathcal{E}_{eff},\, 0.92\,\mathcal{E}_{eff}). \tag{22b}$$

Thus, both analytically modelled (Eq. (21), suffix -M) or data-based approximated (Eq. (22), suffix -DB) two-parameter sets depend only on the low-strain effective Young's modulus $\mathcal{E}_{eff}$ of the homogenised SC. Thus, for either one of these these parameter sets (Eq. (21) or Eq. (22)), the exponential (Eq. (19)) as well as the cubic (Eq. (20)) relationship reduces to a one-parameter model approach for the uni-axial stress-strain behaviour in the strain range up to 1.5. The parameter $\mathcal{E}_{eff}$ has the advantage to be physically meaningful, so that it can be measured from tension testing limited to low-strain loads (up to 0.3). Alternatively, $\mathcal{E}_{eff}$ can be modelled from known stacking characteristics, *i.e.* the composition, geometry and position of each layer in the SCs stack [Ahmad *et al.*, 2021, 2022]. Consequently, the outlined one-parameter non-linear stress-strain ExpCub procedure is efficient as the need for stress-strain measurements is eliminated in the case that $\mathcal{E}_{eff}$ is modelled or limited to the low-strain region ($\varepsilon_t \leq 0.3$ for assessed elastomer SCs, see A) when $\mathcal{E}_{eff}$ is measured. Next, a comparison of the performance of the ExpCub procedure with other stress-strain models, such as the ones outlined in the previous section 2, is presented.

4. Comparison of model performance statistics

Models performance statistics accounting for both their accuracy and their complexity are quantified considering the (adjusted) coefficient of determination $R^2_{(a)}$ and Akaike information criterion AICc as detailed in Appendix B. Performance statistics for the ExpCub procedure and best fit reference models with one ($M = 1$ in Section 4.1), two ($M = 2$ in Section 4.2) or more ($M \geq 3$ in Section 4.3) parameters

Table 1. Overview of median, interquartile minimum and lowest extremum of performance statistics R^2 (in %, rounded to an integer) associated with boxplots in Fig. 1 for best fits outcomes (nH-bf, E-bf, C-bf) and for one-parameter approaches (nH-M, E-M, E-DB, C-M and C-DB). For convenience, model parameters are indicated.

	neo-Hookean (nH-)		exponential (E-)			cubic (C-)		
	nH-bf	nH-M	E-bf	E-DB	E-M	C-bf	C-DB	C-M
parameter(s)	μ	$\mathcal{E}_{eff}$	(A, B)	$\mathcal{E}_{eff}$	$\mathcal{E}_{eff}$	(a, b)	$\mathcal{E}_{eff}$	$\mathcal{E}_{eff}$
median	95	89	99	98	87	99	97	86
interquartile	92	75	99	93	76	99	92	80
extremum	85	47	99	85	62	99	86	66

are compared. Examples of modelled and measured (Appendix A [Ahmad *et al.*, 2023; Van Hirtum *et al.*, 2023]) stress-strain curves $\sigma_t(\varepsilon_t)$ are systematically illustrated for SCs with different $\mathcal{E}_{eff} \leq 65$ kPa (see Fig. 8(b)), *i.e.*, 4.0 kPa, 7.5 kPa, 23.4 kPa and 64.7 kPa.

4.1. *Comparison with one-parameter neo-Hookean model,* $M = 1$

From the reference models listed in Section 2.2, only the neo-Hookean model depends on one parameter, *i.e.*, shear modulus μ. Consequently, model performance statistics of the neo-Hookean model can be seen as a performance benchmark for the one-parameter ExpCub procedure outlined in Section 3.

Boxplots of model accuracy R^2 and Akaike information criterion AICc for the neo-Hookean (nH-· using Eq. (9)) model and the ExpCub procedure applied to either the exponential (E-· using Eq. (19)) or cubic (C-· using Eq. (20)) equation

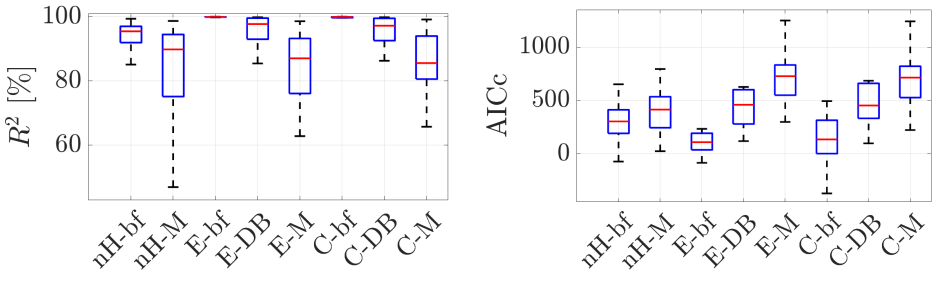

(a) (b)

Fig. 1. Boxplots of performance measures a) R^2 (in %) and b) AICc (a.u.) with median (full line), interquartile range between the first and third quartile (box) and extrema (whiskers) for the Neo-Hookean model for best fit (nH-bf) and modelled (nH-M) parameter values and the ExpCub procedure based on exponential (E-) and cubic (C-) expressions for approximated (modelled (-M) and data-based (-DB)) and best fit (-bf) parameter sets.

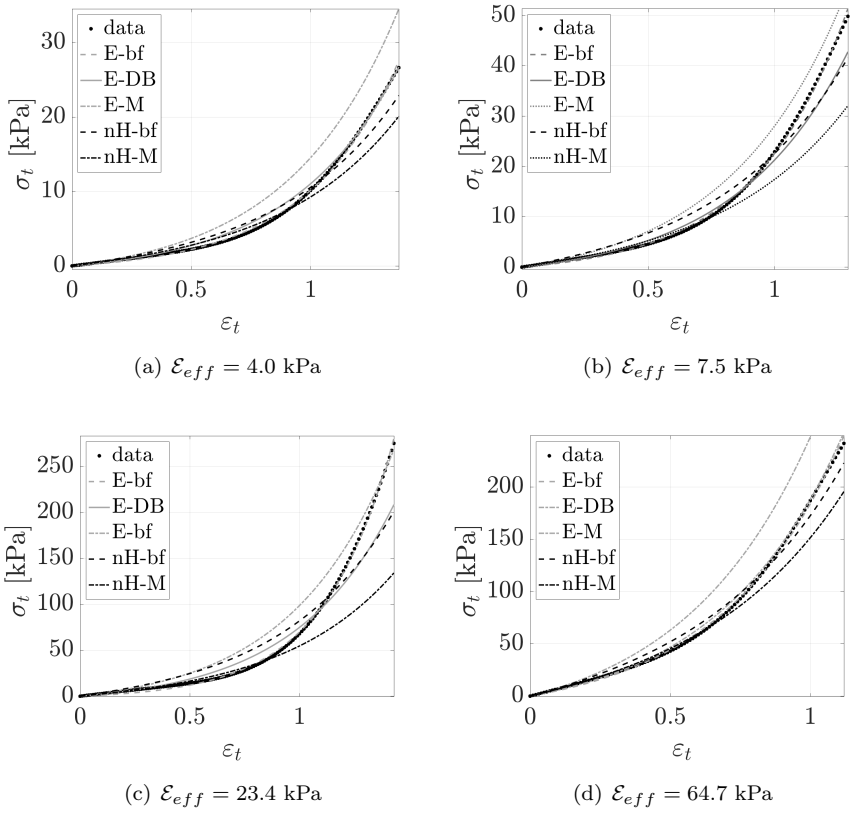

(a) $\mathcal{E}_{eff} = 4.0$ kPa (b) $\mathcal{E}_{eff} = 7.5$ kPa

(c) $\mathcal{E}_{eff} = 23.4$ kPa (d) $\mathcal{E}_{eff} = 64.7$ kPa

Fig. 2. Illustration of measured and estimated stress-stain curves $\varepsilon_t(\sigma_t)$ with Neo-Hookean model for a best fit (nH-bf) and modelled (nH-M) parameter value and the ExpCub procedure based on exponential (E-) expressions for approximated (modelled (-M) and data-based (-DB)) and best fit (-bf) parameter sets: a) $\mathcal{E}_{eff} = 4.0$ kPa, b) $\mathcal{E}_{eff} = 7.5$ kPa, c) $\mathcal{E}_{eff} = 23.4$ kPa, d) $\mathcal{E}_{eff} = 64.7$ kPa.

are plotted in Fig. 1. An overview of boxplots performance statistics R^2 is provided in Table 1 in which medians, interquartile minima and lowest extrema are quantified. The performance of the one-parameter ExpCub procedure is assessed for parameter sets obtained from $\mathcal{E}_{eff}$: *i.e.* analytically modelled sets E-M and C-M (Eq. (21)) and data-based approximated sets E-DB and C-DB (Eq. (22)). For the non-Hookean model, shear modulus μ can also be modelled (nH-M, Eq. (5)) as a function of $\mathcal{E}_{eff}$ using the assumption of isotropy ($\nu = 0.5$). Model performance statistics obtained with best fit parameters (nH-bf, E-bf and C-bf) are shown as well. Examples of modelled and measured stress-strain curves are illustrated in Fig. 2. The exponential (E-bf) and cubic (C-bf) best fit curves require two parameters to be estimated, while the neo-Hookean (nH-bf) best fit curves require one parameter to be estimated. Consequently, two-parameter best fits E-bf and C-bf ($R^2 > 99\%$)

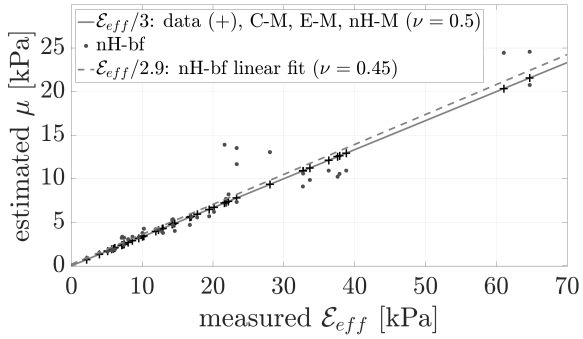

Fig. 3. Estimated shear modulus μ as a function of effective Young's modulus $\mathcal{E}_{eff}$ measured on stress-strain curves of SCs: with isotropy assumption as $\mathcal{E}_{eff}/3$ (full line) from data and modelled curves C-M, E-M and nH-M; neo-Hookean best fit (nH-bf) parameter estimates; $\mathcal{E}_{eff}/2.9$ (dashed line) from a linear fit to best fit parameters.

outperform one-parameter best fit nH-bf ($R^2 > 85\%$, lowest interquartile value 92%, median 95%). Using the modelled instead of the best fit shear modulus μ (nH-M), reduces the neo-Hookean model performance ($R^2 > 47\%$) for which the interquartile R^2-range extents down to 75% and the median yields 89%. This is comparable to the performance obtained for the one-parameter ExpCub procedure with modelled parameters ($R^2 > 62\%$ for E-M and $R^2 > 66\%$ for C-M) as the lowest interquartile minima (76% for E-M and 80% for C-M) and medians (87% for E-M and 86%) have similar values. The performance associated with the one-parameter ExpCub procedure for data based parameters ($R^2 > 85\%$ E-DB and $R^2 > 86\%$ C-DB) on the other hand is comparable to the performance obtained for neo-Hookean best fits (nH-bf) based on the lowest interquartile extrema (93% for E-DB and 92% for C-DB) and medians (98% for E-DB and 97% for C-DB). Consequently, from R^2 follows that the performance of the one-parameter ExpCub procedure is comparable to the performance associated with the one-parameter neo-Hookean model.
This main finding based on R^2 is confirmed considering AICc statistics plotted in Fig. 1(b). Indeed, two-parameter best fits (E-bf and C-bf) yield the lowest values (AICc ≤ 500), intermediate values (AICc ≤ 700) are observed for the neo-Hookean best fit model (nH-bf) and one-parameter ExpCub procedure for data based parameters (E-DB and C-DB) and larger values (AICc ≤ 1300) are associated with one-parameter approaches relying on modelled parameters (nH-M, E-M and C-M). As ExpCub procedure performances obtained using either the cubic or exponential relationship result in comparable performance statistics, in the remaining sections model performance comparison is arbitrarily limited to the exponential relationship (Eq. (19)) and explicit comparison with the cubic relationship is omitted (Eq. (20)).

Under the assumption of isotropy ($\nu = 0.5$), shear modulus μ is approximated (Eq. (5)) as one third of measured $\mathcal{E}_{eff}$ (full line in Fig. 3). As this assumption

Table 2. Overview of median, interquartile minimum and lowest extremum of performance statistics R_a^2 (in %, rounded to one decimal place) associated with boxplots in Fig. 5 for one-parameter approaches (E-M and E-DB) and best fits outcomes (E-bf, Y-bf, G-bf, O-bf and MR-bf). For convenience, model parameters are indicated.

	$M=1$		$M=2$				
	E-M	E-DB	E-bf	Y-bf	G-bf	O-bf	MR-bf
parameter(s)	$\mathcal{E}_{eff}$	$\mathcal{E}_{eff}$	(A,B)	(C_1,C_2)	(μ,J_m)	(μ_1,α_1)	(C_1,C_2)
median	85.6	98.2	99.9	99.6	99.0	99.7	99.6
interquartile	75.3	93.6	99.9	99.5	97.9	99.6	99.2
extremum	62.5	85.3	99.8	99.4	96.3	99.5	98.8

is inherent to the modelled parameter sets, $\mathcal{E}_{eff}/3$ characterises models C-M, E-M and nH-M. The best fit curves with the neo-Hookean model (nH-bf) provide a best fit estimate of the shear modulus for assessed SCs (dots in Fig. 3). A linear fit (fit accuracy $R^2 = 89\%$) to these best fit estimates yields an overall shear modulus estimate $\hat{\mu} = \mathcal{E}_{eff}/2.9$. The corresponding Poisson ratio estimate yields $\hat{\nu} = 0.45$, which is within 4% compared to Poisson ratio $\nu = 0.5$. This shows that the isotropy assumption for elastomer SCs in the assessed conditions (see Appendix A) is reasonable. It is further worthwhile to mention that the estimated value $\hat{\nu} = 0.45$ of the Poisson ratio for assessed elastomer SCs is within range reported in literature for elastomers ($0.35 \leq \nu \leq 0.5$) and silicones ($0.44 \leq \nu \leq 0.9$) [Department, 2003; Murphy *et al.*, 2016; Boretos and Boretos, 2016].

4.2. *Comparison with two-parameter models,* $M = 2$

The performance of the one-parameter ExpCub procedure ($M = 1$) based on exponential expressions with approximated parameter sets (modelled E-M and data-based E-DB) is compared against best fit outcomes (-bf) with two-parameter models ($M = 2$) described in Section 2. Thus, besides best fits for the two-parameter exponential relationship (E-bf, Eq. (19)), also best fits for the Yeoh (Y-bf, Eq. (10)), Gent (G-bf, Eq. (11)), first order Odgen (O-bf, Eq. (13)) and Mooney-Rivlin (MR-bf, Eq. (17)) are considered. Examples of modelled and measured stress-strain curves are illustrated in Fig. 4. As these models depend on a different number of parameters, *i.e.*, $M = 1$ for the ExpCub procedure (E-M and E-DB) and $M = 2$ for best fit estimations with two-parameter models (E-bf, Y-bf, G-bf, O-bf and MR-bf), model accuracies are compared using the adjusted coefficient of determination R_a^2 defined in Eq. (B.3).

Boxplots of model accuracy R_a^2 and Akaike information criterion AICc for the two-parameter models with best fit parameter estimations (E-bf, Y-bf, G-bf, O-bf and MR-bf) are shown in Fig. 5. Boxplots for the one-parameter ExpCub procedure

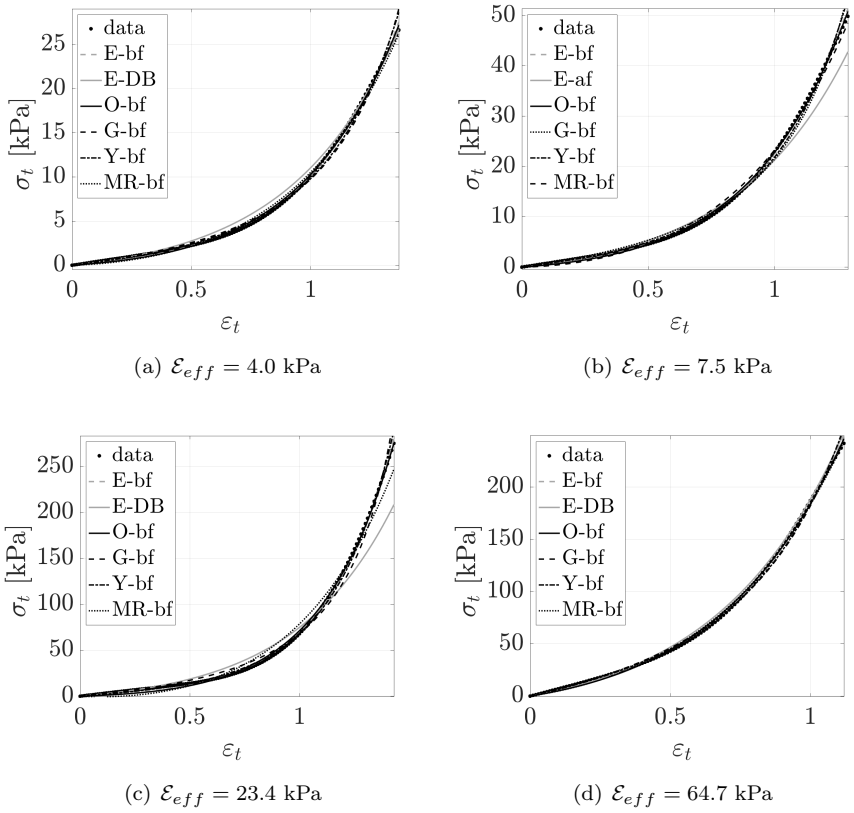

(a) $\mathcal{E}_{eff} = 4.0$ kPa (b) $\mathcal{E}_{eff} = 7.5$ kPa

(c) $\mathcal{E}_{eff} = 23.4$ kPa (d) $\mathcal{E}_{eff} = 64.7$ kPa

Fig. 4. Illustration of measured and estimated stress-stain curves $\varepsilon_t(\sigma_t)$ with the one-parameter ExpCub procedure based on exponential (E-) expressions with approximated parameter set (data-based (E-DB)) and bests fit (-bf) for two-parameter models (E-bf, Y-bf, G-bf, O-bf and MR-bf): a) $\mathcal{E}_{eff} = 4.0$ kPa, b) $\mathcal{E}_{eff} = 7.5$ kPa, c) $\mathcal{E}_{eff} = 23.4$ kPa, d) $\mathcal{E}_{eff} = 64.7$ kPa.

with approximated parameter sets (modelled E-M and data-based E-DB) are plotted for comparison. An overview of boxplots performance statistics R_a^2 is given in Table 2. For all best fit two-parameter models (·-bf including E-bf) $R_a^2 \geq 96\%$ holds as seen on the frame in Fig. 5. Thus, all two-parameter best fit models (·-bf) are more accurate than the one-parameter ExpCub procedure, which agrees with the findings observed for E-bf in the previous Section 4.1. Nevertheless, as previously observed for E-bf in Table 2, the median value for the one-parameter ExpCub procedure ($R_a^2 = 98.2\%$) with data-based parameter approximations (E-DB) approximates the order of magnitude of median values ($R_a^2 \geq 99\%$) quantified for two-parameter best fit models (·-bf). Findings based on R_a^2 are confirmed considering AICc statistics plotted in Fig. 5(b). Furthermore, it is noted that two-parameter best fits with the exponential relationship (E-bf, Eq. (19)) and the Yeoh model (Y-bf, Eq. (10)) result overall in the lowest AICc, although that other two-parameter best fit mod-

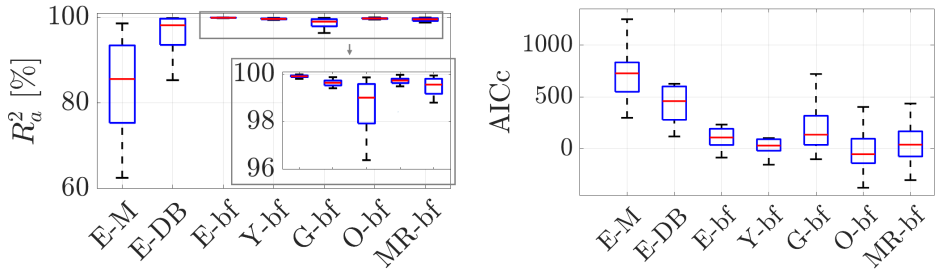

(a) (b)

Fig. 5. Boxplots of performance measures a) R^2 (in %) and b) AICc (a.u.) with median (full line), interquartile range between the first and third quartile (box) and extrema (whiskers) for the one-parameter ExpCub procedure based on exponential (E-) expressions with approximated parameter sets (modelled (E-M) and data-based (E-DB)) and bests fit (-bf) for two-parameter models (E-bf, Y-bf, G-bf, O-bf and MR-bf). A zoom on best fit model performances is framed.

els such as the first order Odgen (O-bf, Eq. (13)) and the Mooney-Rivlin models (MR-bf, Eq. (17)) result in comparable median values.

4.3. *Comparison with multi-parameter models, $M \geq 3$*

In order to assess more generally the performance of reference models on the stress-strain datasets, multi-parameter ($M \geq 3$) models (see Section 2.2) with best fit parameters are assessed as well. The model performance is again quantified considering the adjusted coefficient of determination R_a^2 and the Akaike information criterion AICc in order to account for the different number of model parameters ($3 \leq M \leq 15$). Boxplots of performance measures R_a^2, a zoom in the range $R_a^2 \geq 99.4$ and AICc are shown in Fig. 6(a). For conciseness, the suffix indicating best fit parameters (·-bf) is omitted in the x-axis labels, instead the number of parameters M is explicitly stated after the colon (· : M). As a reference, corresponding boxplots for the two-parameter exponential model with best fit parameters (E-bf indicated as E:2 in Fig. 6) are shown as well. Except for the three-parameter Criscone model (C:3) whose performance in terms of R_a^2 (median $R_a^2 = 97.5\%$) is similar to the one-parameter ExpCub procedure (median $R_a^2 = 98.2\%$ for E-DB in Table 2), all other multi-parameter models are characterised by performance statistics $R_a^2 \geq 99.4\%$ as illustrated in Fig. 6(b). It is observed that increasing the number of parameters, and thus the complexity of the model, does not improve (*e.g.*, for C:3, PS:3 and gMR:3) or at least not significantly improve (*e.g.*, for Y:4, Y:5, O6, O:8) the performance statistics obtained with the best fit two-parameter exponential model (E:2) for which $R_a^2 \geq 99.9\%$ holds. Findings based on R_a^2 are confirmed considering AICc statistics plotted in Fig. 6(c). Examples of modelled and measured stress-strain curves are illustrated in Fig. 7 for two-parameter best fit exponential relationship

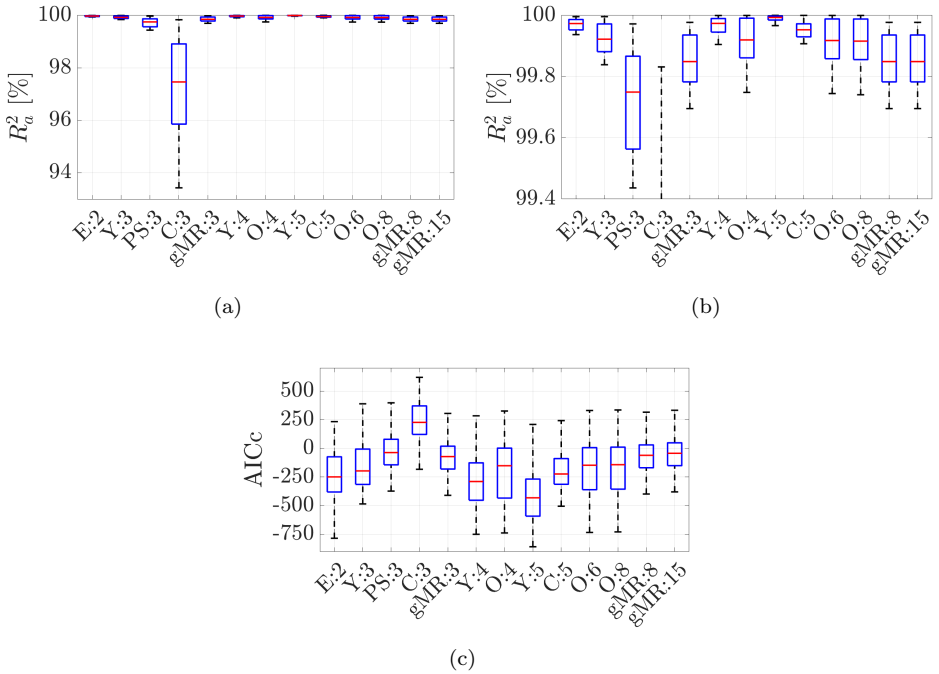

Fig. 6. Boxplots of performance measures R_a^2 (in %) and AICc (a.u.) with median (full line), interquartile range between the first and third quartile (box) and extrema (whiskers) for M-parameter models ($\cdot$:M) with $M \geq 3$ and best fit two-parameter ($M = 2$) exponential model (E:2 or E-bf): a) R_a^2, b) zoom in the range $R_a^2 \geq 99.4\%$, c) AICc.

(E-bf or E:2) and for three-parameter best fits models (PS:3, C:3, Y:3 and gMR:3).

5. Discussion and conclusion

Assessed model performance statistics show that the predictive one-parameter ExpCub procedure with data-based parameter approximations (E-DB or C-DB), as a function of effective low-strain Young's modulus $\mathcal{E}_{eff}$, allows to approximate measured stress-strain curves on SCs for maximum strains between 0.9 and 1.5 with at least the same accuracy ($R^2 \geq 85\%$) as the best fit one-parameter neo-Hookean model. Thus, the ExpCub procedure applied to SCs provides an *a-priori* one-parameter model of measured non-linear stress-strain curves as the ExpCub procedure reflects the excellent best fit accuracy ($R^2 \geq 99\%$, $R_a^2 \geq 99.4\%$) of the underlying exponential and cubic two-parameter relationships compared to reference stress-strain models with up to 15 parameters. In general, it is seen that both from the point of accuracy (R_a^2) as from the point of information criterion (AICc) two-parameter best fit models provide the best balance between goodness of fit and model complexity. Overall, it is concluded that, compared to reference best fit stress-strain models, the

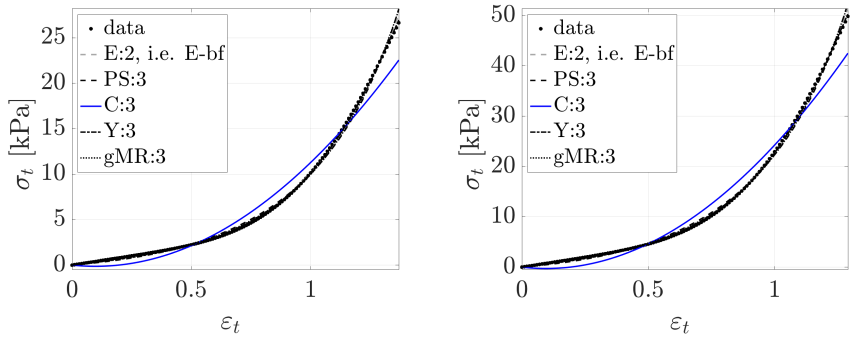

(a) $\mathcal{E}_{eff} = 4.0$ kPa (b) $\mathcal{E}_{eff} = 7.5$ kPa

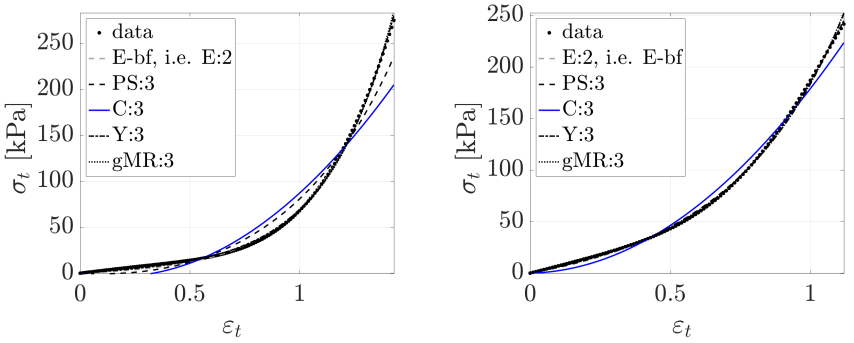

(c) $\mathcal{E}_{eff} = 23.4$ kPa (d) $\mathcal{E}_{eff} = 64.7$ kPa

Fig. 7. Illustration of measured and estimated stress-stain curves $\varepsilon_t(\sigma_t)$ with the best fit exponential relationship with best fit two-parameters (E-bf or E:2) and best fits for three-parameter models (PS:3, C:3, Y:3 and gMR:3): a) $\mathcal{E}_{eff} = 4.0$ kPa, b) $\mathcal{E}_{eff} = 7.5$ kPa, c) $\mathcal{E}_{eff} = 23.4$ kPa, d) $\mathcal{E}_{eff} = 64.7$ kPa.

predictive one-parameter ExpCub procedure provides an accurate approximation of stress-strain behaviour of multi-layer elastomer SCs with the advantage that it relies on a single parameter; *i.e.* the effective low-strain Young's modulus $\mathcal{E}_{eff}$, which is a physical quantity to be either measured from low-strain tension testing or to be estimated analytically when stacking properties are known. Consequently, the analytical ExpCub procedure is accurate as well as efficient for parametric studies of the influence of the stacking structure of elastomer-based SCs under assessed experimental conditions; *i.e.*, strain range up to 1.5, room temperature, elastomer silicone mixtures. This predictive model approach allows for the design and selection of SCs prior to their realisation which contributes to physical studies of fluid-structure interaction as mentioned in the introduction. It is noted that once selected SCs are realised and subjected to stress-strain testing, multi-parameter models can be fitted to the stress-strain data when stress-strain characterisation is aimed for. It is

noted that the current approach for SCs design is limited to linear and non-linear uni-axial stress-strain behaviour, so that other deformations are not accounted for. Although that the approach is extensively evaluated for elastomer-based SCs, other materials could be assessed to consider the approach in a more general context. In this context, it would be of interest to evaluate the generality of the proposed ExpCub procedure on other databases measured by different research groups.

Acknowledgements

Financial support from the CNRS through the 80|Prime program and the Full3DTalkingHead project (ANR-20-CE23-0008-03) is acknowledged.

Appendix

A. Stress-strain SCs data in brief

Stress-strain data curves are measured using uni-axial tension testing at room temperature (21 ± 2 °C, mean and standard deviation) on 22 bone-shaped multi-layer SCs specimens [Ahmad *et al.*, 2023; Van Hirtum *et al.*, 2023]. All specimens have a rectangular test section ($80 \times 19 \times 15$ mm^3), which contains up to five layers with different geometry, composition and stacking orientation (perpendicular, parallel, arbitrary) with respect to the longitudinal direction corresponding to the force direction during tension testing. Layers are molded from elastomer silicone mixtures (either Thinner-Ecoflex (TE) or Thinner-Dragonskin (TD)) with different mass mixing ratios. The linear low-strain region corresponds to $\varepsilon_l \approx 0.3$ or an elongation with 35% in the force direction. All specimens are characterised by an effective low-strain Young's modulus $\mathcal{E}_{eff}$ (Eq. 2) in the range 2-65 kPa and overall value 21 ± 17 kPa (mean and standard deviation). Stress-strain curves are measured for a maximum strain in the range 0.9-1.5 and overall value 1.2 ± 0.2 (mean and standard deviation), which corresponds to an elongation from 150% up to 350%. An overview of the effective low-strain Young's modulus $\mathcal{E}_{eff}$ as a function of the maximum strain ($\max(\varepsilon_t)$) for all assessed SCs is illustrated in Fig. 8(a). All stress-strain data curves contain at least 90 data points so that $90 \leq N \leq 150$ holds for all stress-strain data curves. Measured stress-strain curves $\sigma_t(\varepsilon_t)$ plotted in Fig. 8(b) with different $\mathcal{E}_{eff}$ are used to illustrate the outcome of stress-strain models in Fig. 2, Fig. 4 and Fig. 7.

B. Accuracy measures and information criteria

B.1. *Accuracy measures R^2 and R^2_a*

The accuracy of modelled values $\hat{y}$ with respect to reference data values y is quantified using one of the following accuracy measures: *i.e.* coefficient of determination

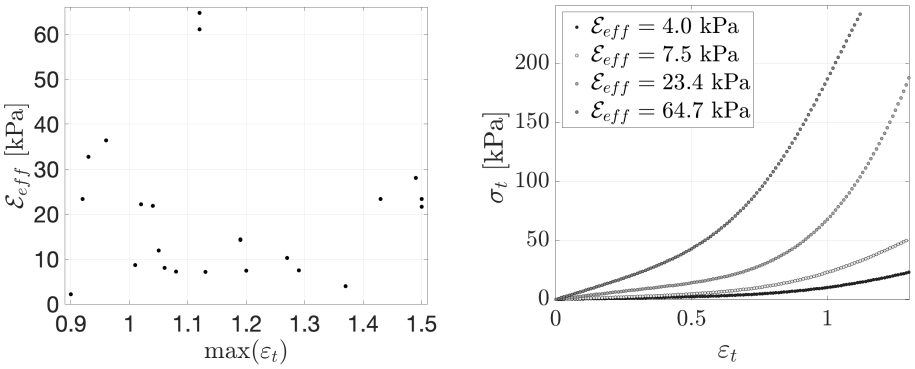

(a) $\mathcal{E}_{eff}(\max(\varepsilon_t))$ (b) examples of $\sigma_t(\varepsilon_t)$

Fig. 8. a) Overview of $\mathcal{E}_{eff}(\max(\varepsilon_t))$ for all assessed SCs, b) Measured stress-strain data $\sigma_t(\varepsilon_t)$ on SCs with $\mathcal{E}_{eff} \leq 65$ kPa used to illustrate model outcomes.

R^2 and adjusted coefficient of determination R_a^2. Note that when measured stress-strain data curves are estimated $y = \sigma_t$ and $\hat{y} = \hat{\sigma}_t$ apply.

The coefficient of determination R^2, defined as

$$R^2 = 1 - \frac{\gamma_{\hat{y}}^2}{\gamma_y^2}, \tag{B.1}$$

is derived from the ratio between the variance of the model residuals $\gamma_{\hat{y}}^2$ and the variance of data γ_y^2 with

$$\gamma_{\hat{y}}^2 = \frac{1}{N}\sum_{i=1}^{N}\left[(\hat{y})_i - \overline{\hat{y}}\,\right]^2 \quad \text{and} \quad \gamma_y^2 = \frac{1}{N}\sum_{i=1}^{N}\left[(y)_i - \overline{y}\right]^2. \tag{B.2}$$

If $\gamma_{\hat{y}}^2 \ll \gamma_y^2$ the measured variance is explained by the model so that R^2 tends towards unity. On the contrary, if $\gamma_{\hat{y}}^2 \approx \gamma_y^2$ then R^2 tends towards zero.

The adjusted coefficient of determination R_a^2 is then defined as a weighted measure of R^2 since

$$R_a^2 = 1 - (1 - R^2)\alpha_a \text{ with } \alpha_a = \frac{N-1}{N-M-1}. \tag{B.3}$$

The weight factor, $\alpha_a \geq 1$, penalises models with many parameters in order to avoid overfitting. Indeed, the factor α_a accounts for the model complexity by considering both the number of parameters M and the number of data points N so that $R_a^2 \leq R^2$ where the equality holds for $\alpha_a = 1$, *i.e.*, when $N \gg M$ as α_a becomes more important for small N and large M.

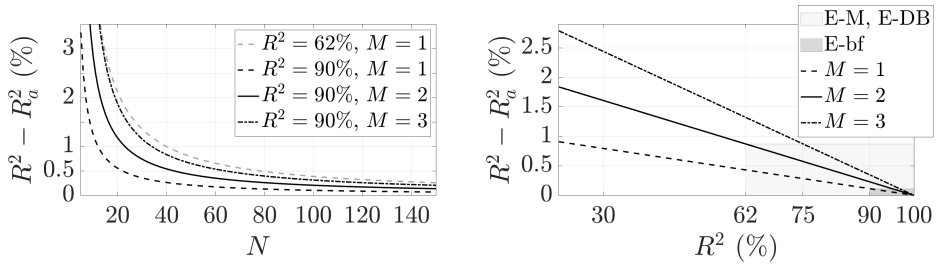

(a) constant R^2: 62% or 90%

(b) constant $N = 90$

Fig. 9. Illustration of $R^2 - R_a^2$ (in %) for models with one ($M = 1$, dashed), two ($M = 2$, full) and three ($M = 3$, dash-dot) parameters as a function of: a) data points N, b) R^2 (in %) for $N = 90$. Values associated with R^2 of interest for the one-parameter ExpCub procedure $R^2 \geq 62\%$ (E-M and E-DB) and for the two-parameter exponential relationship $R^2 \geq 90\%$ (E-bf) are indicated as a reference.

The difference $R^2 - R_a^2 \geq 0$ for models with different number of parameters M ($M = 1$, $M = 2$ and $M = 3$) is illustrated in Fig. 9 as a function of data points N and constant R^2 in Fig. 9(a) and as a function of R^2 and constant N in Fig. 9(b). As a reference, constant values are chosen within the range of interest of assessed stress-strain datasets for which $N \geq 90$ (Appendix A) and for the one-parameter ExpCub procedure ($R^2 \geq 62\%$ for E-M and E-DB in Section 4.1) and for the two-parameter exponential relationship ($R^2 > 90\%$ for E-bf in Section 4.1). It is observed that the influence of N on $R^2 - R_a^2$ is limited to 0.1% for $R^2 \geq 90\%$. Thus, quantifying R_a^2 allows to compare the accuracy of models with a different number of parameters M while the influence of the number of data points N is negligible.

B.2. *Information criteria AICc and BIC*

The Akaike Information Criterion (AIC) is a statistical criterion for model order identification in quantifying the information loss [Akaike, 1974]. In the case of model fitting with least square regression, the AIC is obtained as

$$\mathrm{AIC} = 2M - N \ln \gamma_{\hat{y}}^2 \tag{B.4}$$

where the first model performance term is modified by the second term accounting for the number of parameters M. When comparing different models, the model with the lowest AIC value is the one that explains the greatest amount of variation using the fewest independent variables. For small N the AIC is corrected (AICc) by an additional term as [Hurvich and Tsai, 1989]

$$\mathrm{AICc} = \mathrm{AIC} + \frac{2M(M+1)}{N - M - 1}. \tag{B.5}$$

For large N, the additional term is negligible so that AICc converges to AIC.

A criterion closely related to AICc is the Bayesian information criterion (BIC) obtained as [Schwarz, 1978]

$$\mathrm{BIC} = M \ln N - N \ln \gamma_{\dot{y}}^2. \tag{B.6}$$

Model statistics obtained from AICc and BIC lead to the same findings so that only the AICc is shown in Section 4. For completeness, corresponding figures with BIC statistics are shown in Fig. 10.

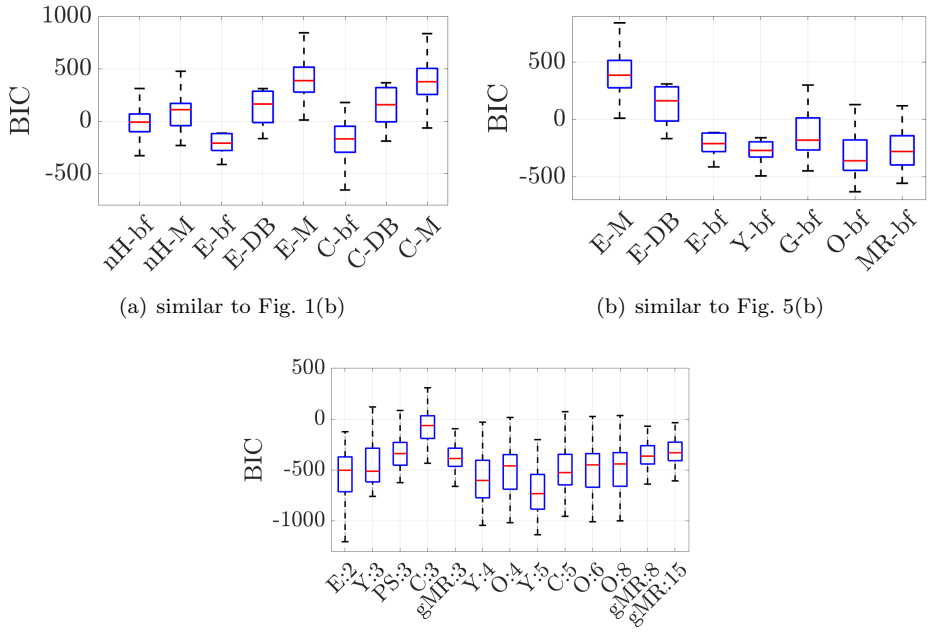

(a) similar to Fig. 1(b)

(b) similar to Fig. 5(b)

(c) similar to Fig. 6(c)

Fig. 10. Boxplots of BIC (a.u.) performance statistics with median (full line), interquartile range between the first and third quartile (box) and extrema (whiskers) for: a) one-parameter models and two-parameter models underlying the ExpCub procedure, b) two-parameter models, c) multi-parameter models ($\cdot$:M) with $M \geq 3$. Boxplots for best fit two-parameter exponential model (E:2 or E-bf) are shown as a reference in each plot.

References

Ahmad, M., Bouvet, A., Pelorson, X. and Van Hirtum, A. [2021] "Modelling and validation of the elasticity parameters of multi-layer specimens pertinent to silicone vocal fold replicas," *Int J Mech Sciences* **208**, 106685.

Ahmad, M., Pelorson, X., Fernández, A., Guasch, O. and Van Hirtum, A. [2022] "Low-strain effective Young's modulus model and validation for multi-layer vocal fold-based silicone specimens with inclusions," *J Appl Phys* **131**, 054701.

Ahmad, M., Pelorson, X., Guasch, O., Fernández, A. and Van Hirtum, A. [2023] "Modelling and validation of the non-linear elastic stress-strain behaviour of multi-layer silicone composites," *J Mech Behav Biomed Mater* **139**, 105690.

Akaike, H. [1974] "A new look at the statistical model identification," *IEEE Trans Automat Control* **19**(6), 716–723.

Alipour, F. and Titze, I. [1991] "Elastic models of vocal fold tissues," *J Acoust Soc Am* **90**, 1326–1331.

Arruda, E. and Boyce, M. [1993] "A three-dimensional constitutive model for the large stretch behavior of rubber elastic materials," *J. Mech. Phys. Solids* **41**(2), 389–412.

Boretos, J. and Boretos, S. [2016] "Biomedical elastomers," *Handbook of biomaterial properties* , 291–337.

Boulanger, P. and Hayes, M. [2001] "Finite-amplitude waves in mooney-rivlin and hadamard materials," in *Topics in finite elasticity* (Springer), pp. 131–167.

Bouvet, A., Tokuda, I., Pelorson, X. and Van Hirtum, A. [2020] "Influence of level difference due to vocal folds angular asymmetry on auto-oscillating replicas," *J. Acoust. Soc.* **147**, 1136–1145.

Bower, A. [2009] *Applied mechanics of solids* (CRC press).

Burks, G., De Vita, R. and Leonessa, A. [2020] "Characterization of the continuous elastic parameters of porcine vocal folds," *J Voice* **34**, 1–7.

Criscione, J., Humphrey, J., Douglas, A. and Hunter, W. [2000] "An invariant basis for natural strain which yields orthogonal stress response terms in isotropic hyperelasticity," *J. Mech. Phys. Solids* **48**(12), 2445–2465.

Demiray, H. [1972] "A note on the elasticity of soft biological tissues," *J Biomech* **5**, 309–311.

Department, C. U. E. [2003] *Materials data book* (Cambridge University Press).

Destrade, M., Saccomandi, G. and Sgura, I. [2017] "Methodical fitting for mathematical models of rubber-like materials," *Proc R Soc A: Math Phys Eng Sci* **473**(2198), 20160811.

Drozdov, A. and Gottlieb, M. [2006] "Ogden-type constitutive equations in finite elasticity of elastomers," *Acta mechanica* **183**, 231–252.

Fu, Y. and Ogden, R. [2001] *Nonlinear elasticity: theory and applications* (Cambridge university press).

Fung, Y. [1967] "Elasticity of soft tissues in simple elongation," *Am J Physiol* **213**, 1605–1624.

Fung, Y. [2010] *Biomechanics* (Springer).

Gent, A. [1996] "A new constitutive relation for rubber," *Rubber chemistry and technology* **69**(1), 59–61.

Gent, A. [2012] *Engineering with rubber: how to design rubber components* (Carl Hanser Verlag GmbH Co KG).

Gou, P. [1970] "Strain energy function for biological tissues," *J. Biomechanics* **3**, 547–550.

Hurvich, C. and Tsai, C. [1989] "Regression and time series model selection in small samples," *Biometrika* **76**(2), 297–307.

Lemaitre, J. [2001] *Handbook of materials behavior models, three-volume set: nonlinear models and properties* (Elsevier).

Marckmann, G. and Verron, E. [2006] "Comparison of hyperelastic models for rubberlike materials," *Rubber Chem and Technol* **79**, 835–858.

Mooney, M. [1940] "A theory of large elastic deformation," *J Appl Phys* **11**(9), 582–592.

Murphy, W., Black, J. and Hastings, G. [2016] *Handbook of biomaterial properties* (Springer).

Murray, P. and Thomson, S. [2012] "Vibratory responses of synthetic, self-oscillating vocal fold models," *J Acoust Soc Am* **132**, 3428–3438.

Odgen, R., Saccomandi, G. and Sgura, I. [2004] "Fitting hyperelastic models to experimental data," *Comp Mech* , 484–502.

Ogden, R. [1997] *Non-linear elastic deformations* (Courier Corporation).

Pucci, E. and Saccomandi, G. [2002] "A note on the gent model for rubber-like materials," *Rubber chemistry and technology* **75**(5), 839–852.

Rivlin, R. [1948] "Large elastic deformations of isotropic materials iv. further developments of the general theory," *Philos Trans R Soc A* **241**(835), 379–397.

Saccomandi, G., Vergori, L. and Zanetti, E. [2022] "Linear, weakly nonlinear and fully nonlinear models for soft tissues: which ones provide the most reliable estimations of the stiffness?" *Philos. Trans. R. Soc. A* **380**(2234), 20210321.

Schwarz, G. [1978] "Estimating the dimension of a model," *Ann Stat* , 461–464.

Taber, L. [2004] *Nonlinear theory of elasticity: applications in biomechanics* (World Scientific).

Tanaka, M., Weisenbach, C., Miller, M. and Kuxhaus, L. [2011] "A continuous method to compute model parameters for soft biological materials," *J Biomed Eng* **133**, 1–7.

Tokuda, I. and Shimamura, R. [2017] "Effect of level difference between left and right vocal folds on phonation: Physical experiment and theoretical study," *J Acoust Soc Am* **142**, 482–492.

Van Hirtum, A., Ahmad, M. and Pelorson, X. [2023] "Uni-axial stress-strain characterisation of silicone composite specimens derived from vocal folds replicas," *European Journal of Mechanics / A Solids* **101**, 105062.

Yeoh, O. [1993] "Some forms of the strain energy function for rubber," *Rubber Chemistry and technology* **66**(5), 754–771.

Zhang, K., Siegmund, T. and Chan, R. [2006] "A constitutive model of the human vocal fold cover for fundamental frequency regulation," *J Acoust Soc Am* **119**, 1050–1062.